Development of Optimization Techniques for Wireless Communication Systems

M.Tech Thesis

by

Anand Kumar

DEPARTMENT OF ELECTRICAL ENGINEERING

INDIAN INSTITUTE OF TECHNOLOGY INDORE

May 2025

Development of Optimization Techniques for Wireless Communication Systems

A THESIS

Submitted in partial fulfillment of the

requirements for the award of the degree

of

Master of Technology

by

Anand Kumar

2302102011

DEPARTMENT OF ELECTRICAL ENGINEERING

INDIAN INSTITUTE OF TECHNOLOGY INDORE

May 2025

INDIAN INSTITUTE OF TECHNOLOGY INDORE

CANDIDATE'S DECLARATION

I hereby certify that the work which is being presented in the thesis entitled **Development of Optimization Techniques for Wireless Communication Systems** in the partial fulfillment of the requirements for the award of the degree of **Master of Technology** and submitted in the **Department of Electrical Engineering, Indian Institute of Technology Indore,** is an authentic record of my own work carried out during the period from July 2023 to June 2025 under the supervision of Prof. Vimal Bhatia, Indian Institute of Technology Indore, India.

I have no interest and will not claim authorship for any work published subsequent to submission of the thesis. I have no objection and have no conflict of interest to the complete (or part) of the work from this guided MTech thesis to be published in the future by thesis supervisors. The copyright is transfered to the thesis supervisor. The matter presented in this thesis has not been submitted by me for the award of any other degree of this or any other institute.

Anand 03/06/2025

Signature of the Student with Date

(Anand Kumar)

This is to certify that the above statement made by the candidate is correct to the best of my knowledge.

03.06.2025

Signature of Thesis Supervisor with Date

(Prof. Vimal Bhatia)

Anand Kumar has successfully given his M.Tech. Oral Examination held on **07/05/2025**.

03.06.2025

Signature(s) of Supervisor(s) of M.Tech. thesis

Date: _____

Saptarshi Ghosh

Convener, DPGC

Date: 03-06-2025

ACKNOWLEDGEMENTS

I would like to take this opportunity to express my deep gratitude to my thesis advisor, **Prof. Vimal Bhatia**, for his exceptional guidance, timely feedback, and continuous encouragement throughout my M.Tech research journey. His mentorship at the *Signals and Systems (SaSg) Lab*, has been invaluable in navigating the challenges of this work and helping me grow as a researcher.

I am also sincerely thankful to **Dr. Keshav Singh**, Associate Professor at National Sun Yat-sen University (NSYSU), Taiwan, for providing me the opportunity to pursue a research internship at the *i-WiC Lab*. The exposure to ongoing international research and his insightful supervision during the internship greatly contributed to shaping the scope and technical depth of this thesis.

I gratefully acknowledge the support provided by **Indian Institute of Technology Indore**, including access to its academic resources and research infrastructure. I would also like to thank the **Ministry of Education, Government of India**, and **NSTC, Taiwan** for the financial assistance that allowed me to pursue my studies without limitations.

Special thanks to my fellow researchers and friends at SaSg Lab, whose constant collaboration, technical discussions, and positive spirit made this experience all the more fulfilling.

Finally, I owe my deepest thanks to my family and close friends, whose unwavering support and encouragement have been the cornerstone of my academic journey.

Anand Kumar

Master of Technology (Communication and Signal Processing)

Roll Number: 2302102011

Indian Institute of Technology Indore

Dedicated to My Family

ABSTRACT

In this study, we investigate advanced optimization strategies for fully connected reconfigurable intelligent surface (FC-RIS) assisted downlink communication systems operating under ultra-reliable low-latency communication (URLLC) constraints. Our focus is on maximizing the finite blocklength (FBL) achievable rate in a multi-user multiple-input single-output (MU-MISO) setting, where joint optimization of beamforming vectors, RIS phase shifts, and blocklength allocation is critical. We address the complexity of the problem arising from high-dimensional search spaces and the presence of Rician fading.

Our investigation begins with a deep learning-based framework that employs gradient-based optimization to handle the non-convexity of the system. We then extend this approach by exploring reinforcement learning methods and employ the twin-delayed deep deterministic policy gradient (TD3) algorithm to jointly optimize active beamforming and blocklength under FC-RIS-aided URLLC scenarios. Unlike earlier works that primarily focused on single connected RIS or standard DDPG methods, our TD3-based approach adapts effectively to the dynamic environment and achieves superior rate and reliability outcomes.

In the final part of our work, we propose a hybrid model that integrates convolutional neural networks (CNN) and long short-term memory (LSTM) networks for initial configuration prediction, followed by refinement using the Successive Convex Approximation (SCA) method. These models demonstrate significant performance gains in terms of throughput and resource utilization compared to traditional techniques. Together, these results affirm the promise of intelligent optimization techniques in next-generation RIS-assisted wireless systems.

Contents

List of Figures

List of Tables

Chapter 1

Introduction

The proliferation of next-generation wireless networks is driven by a range of mission-critical applications including industrial automation, remote healthcare (e.g., telesurgery), and intelligent transportation systems. These applications necessitate stringent communication requirements, characterized primarily by **ultra-reliable and low-latency communication (URLLC)**. URLLC, one of the three service categories defined in 5G by 3GPP, demands end-to-end latencies below 1 millisecond and reliability greater than 99.999% [1].

Traditional communication systems, based on Shannon's asymptotic capacity theorems, assume large blocklengths and do not cater well to short-packet transmissions. In contrast, URLLC scenarios require short packet sizes, necessitating analysis under the **finite blocklength (FBL)** regime. In the FBL regime, throughput is significantly affected by decoding error probability, blocklength, and channel dispersion, making optimization and resource allocation more challenging [2].

1.1 Key Technologies for URLLC

1.1.1 Non-Orthogonal Multiple Access (NOMA)

NOMA has emerged as a key enabler for high spectral efficiency in URLLC networks. Unlike orthogonal access schemes, NOMA allows multiple users to share the same frequency/time resources by employing power-domain or code-domain separation. In **power-domain NOMA**, different power levels are allocated to users, and successive interference cancellation (SIC) is used at the receiver for decoding. This concurrent access boosts system throughput and enables better support for heterogeneous QoS demands [3].

1.1.2 Reconfigurable Intelligent Surfaces (RIS)

RIS is a novel physical-layer technology that enhances the controllability of wireless environments. An RIS consists of a large number of low-cost passive elements that can independently reflect incident signals with adjustable phase shifts. These surfaces can intelligently reshape the wireless propagation environment to improve coverage, signal strength, and interference mitigation [4, 5].

In particular, **Fully Connected RIS (FC-RIS)** differs from the more common **Single Connected RIS (SC-RIS)** by enabling connections among all reflective elements. This provides a much higher degree of control and greater flexibility in shaping waveforms, which is especially advantageous in multi-user scenarios under URLLC constraints. However, it also increases the dimensionality and complexity of the system optimization problem.

1.2 Optimization in Wireless Communication Systems

1.2.1 The Need for Joint Optimization

Modern wireless communication systems are increasingly complex, involving multiple interdependent components such as transmitters, receivers, relays, antennas, and intelligent surfaces. Optimal system performance requires the joint configuration of several parameters, including:

- **Beamforming vectors** for managing signal strength and interference,
- **Resource allocation** across time, frequency, and spatial domains,
- **Power control and user scheduling** for fairness and throughput maximization,
- **Intelligent surface tuning**, such as phase shift control in RIS-assisted systems.

These parameters are often coupled through the underlying channel dynamics and user demands. Therefore, efficient *joint optimization* becomes essential for achieving high spectral efficiency, coverage reliability, and energy efficiency. However, these optimization problems are typically non-linear, non-convex, and high-dimensional, especially in multi-user and multi-antenna systems.

1.2.2 Traditional Optimization Approaches

Historically, wireless system optimization has relied on model-driven approaches based on well-defined mathematical formulations. Some of the most common tools include:

- **Convex optimization**, which allows for efficient and globally optimal solutions when the problem can be relaxed to a convex form,
- **Successive Convex Approximation (SCA)**, which iteratively approximates non-convex problems as solvable convex subproblems,
- **Semidefinite Relaxation (SDR)**, often used in beamforming and power control,
- **Alternating Optimization**, where variables are optimized in a sequential manner while others are held fixed.

While these techniques are mathematically sound, they suffer from limitations when applied to practical large-scale or dynamic systems. These include high computational complexity, dependence on perfect channel state information (CSI), and difficulty adapting to real-time variations.

1.2.3 Emergence of Learning-Based Optimization

With the growth of data availability and computational power, learning-based methods—particularly **deep learning (DL)** and **reinforcement learning (RL)**—have shown great promise in addressing the limitations of traditional methods.

1.2.3.0.1 Deep Learning (DL): Supervised and unsupervised DL models can learn non-linear mappings between CSI and control variables such as beamforming vectors or power levels. Convolutional Neural Networks (CNN), Long Short-Term Memory networks (LSTM), and multi-layer perceptrons (MLP) have been applied in

scenarios such as channel estimation, modulation classification, and resource allocation [6].

1.2.3.0.2 Reinforcement Learning (RL): In contrast to supervised DL, RL does not require labeled data. It learns optimal decision policies through trial and error interactions with the environment. Algorithms such as Q-learning, Deep Q-Network (DQN), and Twin Delayed Deep Deterministic Policy Gradient (TD3) have been used to optimize scheduling, power allocation, and phase shifts in RIS-aided systems [7].

1.2.3.0.3 Advantages and Challenges: Learning-based methods offer strong adaptability, scalability, and the ability to operate with partial or outdated CSI. However, they also bring challenges such as training instability, generalization across environments, and the need for large datasets or exploration time.

1.2.4 Summary

Optimization in wireless systems has evolved from purely analytical methods to hybrid and data-driven approaches. While traditional optimization remains essential for interpretability and convergence guarantees, learning-based frameworks offer flexibility and scalability that are well-suited for modern wireless environments. A growing body of research is now focused on combining both paradigms to achieve robust and efficient wireless system optimization.

1.3 Thesis Objective and Contributions

This thesis addresses the above challenges by proposing two complementary DL-based optimization frameworks tailored for FC-RIS-assisted short packet NOMA systems in the FBL regime:

1. A **hybrid CNN-LSTM and SCA** framework that uses deep learning to initialize the RIS phase matrix and applies model-based convex optimization for beamforming and blocklength.

2. A **fully gradient-based optimization** approach using the Adam optimizer and a neural network trained to maximize the system reward (sum FBL rate).

The main contributions of this work are:

- Development of a comprehensive system model incorporating Rician fading, FC-RIS architecture, and URLLC-FBL constraints.

- Formulation of a joint optimization problem for RIS phase shifts, BS beamforming, and user-specific blocklengths.

- Design of a hybrid deep learning and optimization framework that efficiently balances performance and complexity.

- Design of a gradient-based DL framework that jointly optimizes all critical parameters using a fully connected neural network.

- Extensive simulation and complexity analysis demonstrating the superiority of the proposed methods over baseline schemes including SC-RIS, ZF, and random phase strategies.

The complete implementation code, simulations, and result visualizations associated with this thesis are publicly available at: `https://github.com/anandk3198/MTech_Thesis`. This repository serves as a supplementary material for reproducibility and further research.

1.4 Thesis Organization

The remainder of this thesis is organized as follows:

- **Chapter 2:** Literature review covering RIS architectures, NOMA, and optimization methods for URLLC systems.
- **Chapter 3:** Detailed system model and mathematical formulation of the optimization problem.
- **Chapter 4:** Gradient-based deep learning model for joint parameter optimization.
- **Chapter 5:** Proposed CNN-LSTM and SCA-based hybrid optimization algorithm.
- **Chapter 6:** Simulation setup, performance evaluation, and complexity analysis.
- **Chapter 7:** Conclusion and directions for future research.

Chapter 2

Literature Survey

The deployment of RIS in wireless communication systems has garnered significant attention in recent years due to its potential to enhance spectral efficiency, reliability, and security in complex communication environments. The integration of RIS in URLLC systems, especially in scenarios involving short packet communications, has led to the exploration of various approaches for optimizing system performance. This section reviews the existing literature on RIS-aided communication systems, with a focus on related challenges and proposed solutions.

2.1 Reconfigurable Intelligent Surfaces

Reconfigurable Intelligent Surfaces have emerged as a transformative technology for next-generation wireless networks. RIS can dynamically control the electromagnetic environment by adjusting the phase shifts of passive elements. Early works like [8, 9, 5] laid the foundation for energy-efficient and programmable wireless propagation.

The comprehensive tutorial by Zhang and Zhang [10] provides a taxonomy of RIS configurations (single-connected, group-connected, fully-connected), deployment models, and optimization frameworks. Li et al. [11] advanced this understanding

by contrasting diagonal versus FC-RIS, showing superior performance at the cost of higher design complexity.

2.2 Finite Blocklength and URLLC Communication

Short packet communication under the FBL regime is vital for URLLC. The foundational work by Polyanskiy et al. [2] introduced the mathematical framework for analyzing channel capacity in the FBL regime. Subsequent system-level analyses such as [12, 13] focused on the latency-reliability trade-offs and how resource allocation must change in short-packet transmission scenarios.

Hashemi et al. [14] studied the interplay between blocklength and achievable rates in RIS-aided short packet systems, proposing joint sum-rate and blocklength optimization strategies.

2.3 RIS-Aided URLLC Systems

The integration of RIS with URLLC systems has been explored in recent works like [15, 16]. These studies demonstrate how RIS can enhance reliability and compensate for poor direct links under strict latency constraints. The work by Kurma et al. [17] introduced an active RIS model for digital twin-based URLLC IoT networks and compared fully-connected versus sub-connected architectures.

Zhu et al. [18] proposed gradient-based manifold meta-learning for beamforming under RIS-aided communication, effectively balancing reliability and complexity in URLLC scenarios.

2.4 Deep Learning and Reinforcement Learning in Wireless Optimization

With the increasing complexity of wireless environments, model-free and learning-based optimization has gained prominence. Dai et al. [19] presented DL as a paradigm shift in wireless optimization. CNN and LSTM models, as utilized in [20], demonstrated effective CSI estimation in RIS-NOMA systems.

RL-based schemes like those in [21, 16] employed TD3 and actor-critic models for RIS phase control and blocklength adaptation under uncertain and dynamic conditions.

2.5 Multi-Objective and Joint Optimization Techniques

Several works have addressed the challenge of optimizing multiple objectives simultaneously — e.g., rate, reliability, latency, and energy. Marler and Arora [22] provide a survey of multi-objective optimization methods relevant across engineering disciplines. In the context of RIS and NOMA, joint beamforming, power allocation, and blocklength optimization is addressed in works like [23, 24, 25], which highlight both algorithmic strategies and system trade-offs.

2.6 Research Gap, Motivation, and Contributions

2.6.1 Research Gap

The existing body of research on RIS-aided wireless systems has predominantly focused on two separate fronts: (i) SC-RIS architectures, and (ii) NOMA in isolation.

While SC-RIS has gained popularity due to its simplicity and lower hardware cost, it falls short in complex multi-user environments where interference mitigation and fine-grained control are paramount.

Moreover, most of the works targeting URLLC under FBL constraints either consider conventional orthogonal access or optimize one subset of system parameters—such as transmit power or phase shift—while neglecting joint optimization. Studies that do incorporate machine learning methods often rely on basic reinforcement learning techniques like Deep Deterministic Policy Gradient (DDPG) [16], or they address phase shift design independently from blocklength and beamforming [21].

To date, no comprehensive solution has been proposed that leverages the high degrees of freedom offered by FC-RIS in a short-packet NOMA setting, while simultaneously optimizing beamforming, RIS phase shifts, and blocklength under stringent URLLC constraints.

2.6.2 Motivation

FC-RIS introduces a transformative approach to wireless channel control by interconnecting all passive elements, offering enhanced phase resolution and spatial diversity. This makes FC-RIS particularly suitable for URLLC scenarios, which demand ultra-low latency and extremely high reliability. However, this architectural advantage comes at the cost of significant computational and optimization complexity, particularly in high-dimensional and non-convex problem spaces.

Traditional convex optimization methods struggle to scale under such complexity, and while DL offers high adaptability and performance in high-dimensional spaces [19], most existing DL-based solutions do not account for the interdependence

between all optimization variables—beamforming, blocklength, and RIS configuration—simultaneously.

Thus, there is a critical need to develop hybrid and data-driven optimization frameworks that can fully exploit the benefits of FC-RIS while satisfying the rigorous constraints imposed by URLLC applications.

2.6.3 Contributions

In light of the identified research gap and optimization challenges, this thesis makes the following key contributions:

- **Comprehensive Joint Optimization Framework:** We formulate a new optimization problem that aims to maximize the sum FBL rate in an FC-RIS-aided short packet NOMA system. The problem jointly considers beamforming at the base station, phase shift configuration of the FC-RIS, and blocklength allocation, under URLLC constraints.

- **Use of TD3 for FC-RIS Optimization:** Drawing from recent reinforcement learning applications [21], we apply the TD3 algorithm to simultaneously optimize beamforming and blocklength in FC-RIS-aided NOMA under FBL, making this one of the first applications of TD3 in such a context.

- **Gradient-Based Deep Learning Framework:** A second framework employs a gradient-based learning approach, using the Adam optimizer to iteratively update all system parameters. This is complemented by a feed-forward neural network trained to optimize blocklength allocation based on channel features, inspired by the manifold meta-learning concept [18].

- **Hybrid Deep Learning and SCA Approach:** We propose a hybrid optimization strategy that integrates a CNN-LSTM model for real-time RIS configuration prediction with a model-based SCA method for beamforming and blocklength refinement. This balances performance with computational efficiency.

- **Empirical Validation and Complexity Analysis:** Through simulations, we validate our proposed methods against baseline models including SC-RIS, random phase shift, and zero-forcing beamforming. We also provide a detailed computational complexity analysis to understand the trade-offs in performance and scalability.

The proposed methods offer a significant step forward in realizing intelligent, adaptive, and robust FC-RIS-aided NOMA systems suitable for future URLLC wireless networks.

Chapter 3

System Model and Problem Formulation

3.1 System Architecture

We consider a multi-user downlink short-packet communication system designed for URLLC. The system architecture consists of a base station (BS) equipped with M antennas arranged in a uniform planar array (UPA), K single-antenna user equipments (UEs), and a FC-RIS comprising N passive reflecting elements. The FC-RIS acts as a smart and tunable reflector positioned between the BS and the UEs to assist in overcoming channel impairments such as deep fading or blockage, which are critical in high-reliability environments.

Each UE receives its intended signal through both direct BS-to-UE links and indirect RIS-assisted paths. The system utilizes NOMA to enable simultaneous service to all UEs over the same time and frequency resources, thereby improving spectral efficiency. The overall architecture is illustrated in Fig. 3.1.

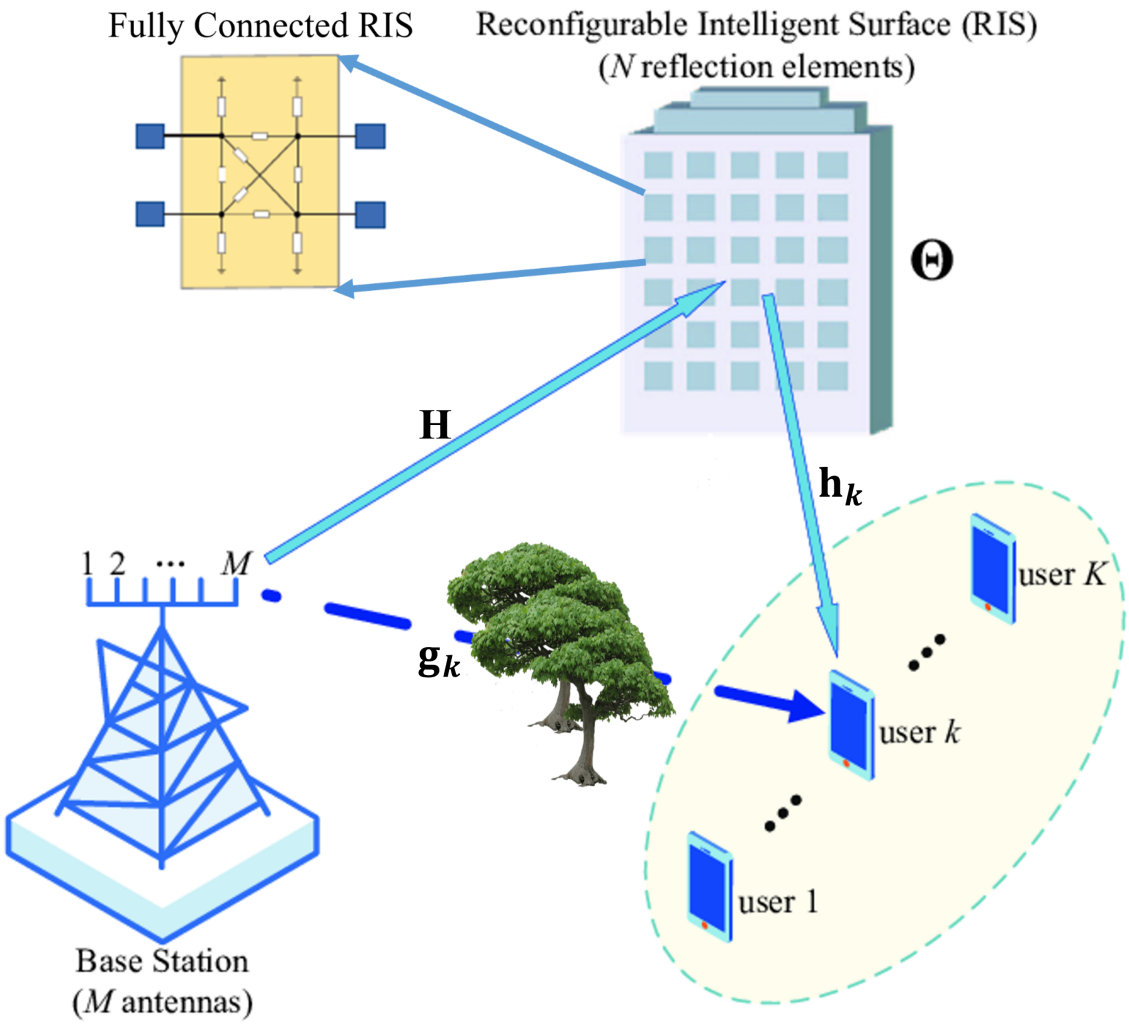

Figure 3.1: System Model: A multi-antenna multi-user short packet communication network with Fully Connected RIS.

3.1.1 Signal Transmission and Power Constraint

The signal transmitted from the BS is a linear combination of data symbols intended for different users, modulated by their respective beamforming vectors:

$$\mathbf{x} = \sum_{k=1}^{K} \mathbf{w}_k s_k, \tag{3.1}$$

where $\mathbf{w}_k \in \mathbb{C}^{M\times 1}$ is the beamforming vector for user k, and s_k is the corresponding transmitted symbol with unit power, i.e., $\mathbb{E}[|s_k|^2] = 1$.

The total transmit power from the BS is constrained by:

$$\mathrm{tr}(\mathbf{W}\mathbf{W}^H) = \sum_{k=1}^{K} \|\mathbf{w}_k\|^2 \leq P_{\text{total}}, \tag{3.2}$$

where $\mathbf{W} = [\mathbf{w}_1, \ldots, \mathbf{w}_K]$ and P_{total} denotes the maximum allowable transmission power.

3.2 Channel Model

We consider three types of channels in the system:

1. Direct channel from BS to user k: $\mathbf{g}_k \in \mathbb{C}^{M\times 1}$,
2. BS-to-RIS channel: $\mathbf{H} \in \mathbb{C}^{N\times M}$,
3. RIS-to-user k channel: $\mathbf{h}_k \in \mathbb{C}^{N\times 1}$.

Each of these channels is modeled using Rician fading to capture the contributions of both line-of-sight (LoS) and non-line-of-sight (NLoS) components. Specifically, the direct channel is modeled as:

$$\mathbf{g}_k = \sqrt{\frac{\zeta_k}{\zeta_k + 1}}\mathbf{g}_{\text{LoS},k} + \sqrt{\frac{1}{\zeta_k + 1}}\tilde{\mathbf{g}}_{\text{NLoS},k}, \tag{3.3}$$

where ζ_k is the Rician factor for user k, $\mathbf{g}_{\text{LoS},k}$ represents the deterministic LoS component, and $\tilde{\mathbf{g}}_{\text{NLoS},k} \sim \mathcal{CN}(0, \beta_k \mathbf{I})$ is the NLoS component.

3.3 FC-RIS Design and Scattering Matrix

3.3.1 Definition and Properties

The FC-RIS is characterized by a reconfigurable impedance network where each element is connected to all others through tunable reactances. This configuration is

modeled using a scattering matrix $\mathbf{\Theta}$ derived from network theory. Following the analysis in [26], the FC-RIS matrix is expressed as:

$$\mathbf{\Theta} = (j\mathbf{X} + Z_0\mathbf{I})^{-1}(j\mathbf{X} - Z_0\mathbf{I}), \tag{3.4}$$

$$\text{subject to:} \quad \mathbf{X} = \mathbf{X}^T, \tag{3.5}$$

where $\mathbf{X} \in \mathbb{R}^{N\times N}$ is the symmetric reactance matrix and Z_0 is the reference impedance. These constraints ensure $\mathbf{\Theta}$ is unitary and symmetric: $\mathbf{\Theta}^H\mathbf{\Theta} = \mathbf{I}$, $\mathbf{\Theta} = \mathbf{\Theta}^T$.

3.3.2 Signal Reception and SINR

The signal received at user k is:

$$y_k = (\mathbf{g}_k^H + \mathbf{h}_k^H\mathbf{\Theta}\mathbf{H})\sum_{i=1}^{K}\mathbf{w}_i s_i + z_k, \tag{3.6}$$

where $z_k \sim \mathcal{CN}(0, \sigma^2)$ is AWGN. The SINR at user k is therefore given by:

$$\text{SINR}_k = \frac{|(\mathbf{g}_k^H + \mathbf{h}_k^H\mathbf{\Theta}\mathbf{H})\mathbf{w}_k|^2}{\sum_{i\neq k}|(\mathbf{g}_k^H + \mathbf{h}_k^H\mathbf{\Theta}\mathbf{H})\mathbf{w}_i|^2+\sigma^2}. \tag{3.7}$$

3.4 Finite Blocklength Transmission Model

In URLLC scenarios, FBL coding must be employed, which requires a departure from the Shannon capacity framework. The rate achievable by user k under blocklength c_k and target error probability ϵ_k is given by [2]:

$$R_k = c_k \log_2(1 + \text{SINR}_k) - Q^{-1}(\epsilon_k)\sqrt{c_k V(\text{SINR}_k)} + \log_2(c_k), \tag{3.8}$$

where the channel dispersion $V(\text{SINR}_k)$ is:

$$V(\text{SINR}_k) = \frac{1}{(\ln 2)^2}\left(1 - \frac{1}{(1 + \text{SINR}_k)^2}\right). \tag{3.9}$$

3.5 Optimization Problem Formulation

Our goal is to jointly optimize the beamforming matrix $\mathbf{W}$, the FC-RIS scattering matrix $\mathbf{\Theta}$, and the blocklength vector $\mathbf{c} = [c_1, \ldots, c_K]$ to maximize the total FBL throughput. The formal optimization problem is:

$$\begin{aligned}
&\max_{\mathbf{W},\mathbf{\Theta},\mathbf{c}} \sum_{k=1}^{K} \left[c_k \log_2(1 + \mathrm{SINR}_k) + \log_2(c_k) - Q^{-1}(\epsilon_k^{\mathrm{th}}) \sqrt{c_k V(\mathrm{SINR}_k)} \right] \\
&\text{subject to:} \quad \mathbf{\Theta} = (j\mathbf{X} + Z_0\mathbf{I})^{-1}(j\mathbf{X} - Z_0\mathbf{I}), \\
&\qquad \mathbf{X} = \mathbf{X}^T, \\
&\qquad \sum_{k=1}^{K} \|\mathbf{w}_k\|^2 \leq P_{\mathrm{total}}, \\
&\qquad \sum_{k=1}^{K} c_k \leq C, \quad c_k \geq c_{\min}, \quad \forall k.
\end{aligned} \tag{3.10}$$

This optimization framework is designed to maximize the FBL transmission rate while satisfying the stringent reliability and latency constraints imposed by URLLC. The associated constraints are described as follows:

- C1: Ensures the scattering matrix $\mathbf{\Theta}$ is defined based on the reactance matrix $\mathbf{X}$ and the reference impedance Z_0, adhering to the physical characteristics of the RIS.
- C2: Imposes that the matrix $\mathbf{X}$ is symmetric, reflecting the practical phase-shift model that affects the amplitude response of the RIS.
- C3: Limits the total transmit power at the BS to P_{total}, ensuring compliance with power efficiency and hardware constraints.
- C4: Restricts the total number of channel blocklengths c_k across all UEs to a maximum value C, ensuring each c_k meets the minimum requirement $c_{\min}$ to maintain the validity of the FBL regime rate.

3.5.1 RIS Cascaded Channel Representation

A vector $\boldsymbol{\theta}$ is derived by vectorizing the $N \times N$ FC-RIS scattering matrix $\boldsymbol{\Theta}$ using the approach proposed in [27]. This cascaded channel through the RIS is expressed using the vectorized form of the scattering matrix:

$$\mathbf{a}_k = \boldsymbol{\theta}_{N^2 \times 1} \cdot \mathbf{A}_k \cdot \mathbf{H}, \tag{3.11}$$

$$\mathbf{A}_k = \left[\mathbf{J}_0 \tilde{\mathbf{h}}_k, \mathbf{J}_N \tilde{\mathbf{h}}_k, \ldots, \mathbf{J}_{(N-1)N} \tilde{\mathbf{h}}_k \right], \tag{3.12}$$

$$\tilde{\mathbf{h}}_k = \begin{bmatrix} \mathbf{h}_k^H \\ \mathbf{0}_{(N-1)N}^T \end{bmatrix}, \quad \mathbf{J} = \begin{bmatrix} \mathbf{0}_{N^2-1}^T & 0 \\ \mathbf{I}_{N^2-1} & \mathbf{0}_{N^2-1} \end{bmatrix}. \tag{3.13}$$

This joint optimization problem is highly non-convex due to the interdependence of variables in the SINR, the presence of non-linear functions such as $Q^{-1}(\cdot)$, and the structural constraints on $\boldsymbol{\Theta}$. Additionally, the FC-RIS offers a much larger control space than traditional SC-RIS, making conventional optimization methods computationally intractable. Therefore, hybrid techniques involving model-based and learning-based algorithms are essential for achieving efficient real-time configuration.

Chapter 4

Gradient-Based Deep Learning Optimization

4.1 Overview

This chapter presents a gradient-based DL framework aimed at jointly optimizing the beamforming matrix, RIS scattering matrix, and blocklength allocation for each user in a multi-user FC-RIS-aided MIMO URLLC system. The proposed framework builds upon differentiable reward-driven optimization and integrates it with a deep neural network for post-refinement of communication parameters.

The optimization objective is to enhance the system sum-rate while satisfying URLLC constraints, using gradients of a differentiable performance metric. This method efficiently updates all critical parameters via backpropagation and gradient descent.

4.2 Gradient-Based Joint Optimization

4.2.1 System Initialization and Optimization Flow

Initially, the beamforming matrix $\mathbf{W} \in \mathbb{C}^{M\times K}$, RIS scattering matrix $\mathbf{\Theta} \in \mathbb{C}^{N\times N}$, and user blocklengths $\mathbf{c} = [c_1, \ldots, c_K]$ are randomly initialized or heuristically set. At each iteration, the algorithm proceeds with the following steps:

4.2.2 SINR and FBL Rate Calculation

For each user k, the effective SINR is calculated using the expression:

$$\mathrm{SINR}_k = \frac{|(\mathbf{g}_k^H + \mathbf{h}_k^H \mathbf{\Theta} \mathbf{H})\mathbf{w}_k|^2}{\sum_{i\neq k} |(\mathbf{g}_k^H + \mathbf{h}_k^H \mathbf{\Theta} \mathbf{H})\mathbf{w}_i|^2 + \sigma^2}, \tag{4.1}$$

where $\mathbf{w}_k$ is the beamforming vector for user k, and the interference is summed over all $i \neq k$.

The achievable FBL rate R_k is then computed using:

$$R_k = c_k \log_2(1 + \mathrm{SINR}_k) - Q^{-1}(\epsilon_k)\sqrt{c_k V(\mathrm{SINR}_k)} + \log_2(c_k), \tag{4.2}$$

where ϵ_k is the target error probability, and $V(\mathrm{SINR}_k)$ is the channel dispersion.

The cumulative system reward is defined as the sum of achievable rates:

$$R = \sum_{k=1}^{K} R_k. \tag{4.3}$$

4.2.3 Gradient-Based Parameter Updates

Guided by the GMML approach [18], the gradients of the system reward R are used to iteratively update:

- Beamforming matrix $\mathbf{W}$: $\nabla_{\mathbf{W}} R$
- RIS matrix $\mathbf{\Theta}$: $\nabla_{\mathbf{\Theta}} R$

- Blocklength vector $\mathbf{c}$: $\nabla_{\mathbf{c}} R$

All updates are performed using the Adam optimizer with gradient clipping to avoid numerical instability:

$$\mathbf{W}^{(t+1)} = \text{Adam}(\mathbf{W}^{(t)}, \nabla_{\mathbf{W}} R), \tag{4.4}$$

$$\mathbf{\Theta}^{(t+1)} = \text{Adam}(\mathbf{\Theta}^{(t)}, \nabla_{\mathbf{\Theta}} R), \tag{4.5}$$

$$\mathbf{c}^{(t+1)} = \text{Adam}(\mathbf{c}^{(t)}, \nabla_{\mathbf{c}} R). \tag{4.6}$$

The optimization continues until convergence is achieved, ensuring the optimal values for $\mathbf{W}$ and $\mathbf{\Theta}$.

4.3 Deep Learning-Based Blocklength and Resource Refinement

The neural network model is designed to predict the reward r_0, which guides the optimization of blocklength and resource allocation. The architecture consists of an input layer, three hidden layers, and an output layer, as illustrated in Fig. 4.1.

4.3.1 Problem Motivation and Architecture

Once $\mathbf{W}$ and $\mathbf{\Theta}$ are optimized, a DL model is employed to refine blocklength allocation and further enhance the system reward. The model is trained on system state features extracted from optimized configurations.

4.3.1.1 Input Features

Each sample in the dataset contains the following:

- **State 1:** Initial interference power and phase.

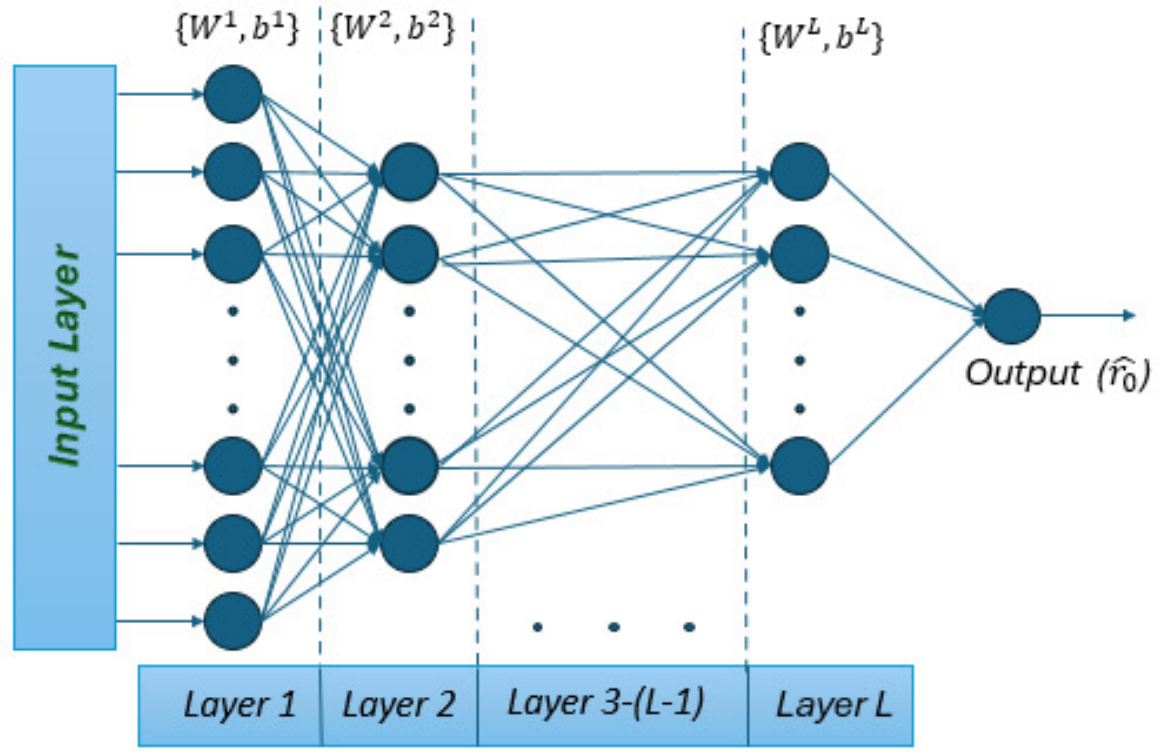

Figure 4.1: Neural Network Architecture

- **State 2:** Norms of channel vectors, beamforming matrix statistics.
- **State 3:** RIS phase shift parameters $\boldsymbol{\theta}$.

4.3.1.2 Feature Normalization

Each input feature x_i is normalized using z-score:

$$x_i^{\text{norm}} = \frac{x_i - \mu_i}{\sigma_i}, \tag{4.7}$$

where μ_i and σ_i are the mean and standard deviation of the i-th feature.

4.3.2 Network Architecture and Training

The neural network is designed to predict the system reward $\hat{r}_0$, which reflects the overall performance in terms of achievable rate under finite blocklength constraints.

The model takes as input a normalized feature vector $\mathbf{x} \in \mathbb{R}^n$, comprising the system state information such as interference metrics, power allocations, RIS phase shifts, and channel properties. The input is passed through a deep feedforward neural network consisting of three hidden layers, each followed by a ReLU activation and dropout regularization to prevent overfitting.

The first hidden layer applies a linear transformation followed by a non-linear activation, computed as:

$$\mathbf{h}^{(1)} = \text{ReLU}(\boldsymbol{\Omega}_1 \mathbf{x} + \boldsymbol{\beta}_1), \tag{4.8}$$

where $\boldsymbol{\Omega}_1 \in \mathbb{R}^{256 \times n}$ is the weight matrix, $\boldsymbol{\beta}_1 \in \mathbb{R}^{256}$ is the bias vector, and ReLU denotes the element-wise rectified linear unit activation function.

The second hidden layer further processes the intermediate representation:

$$\mathbf{h}^{(2)} = \text{Dropout}\left(\text{ReLU}(\boldsymbol{\Omega}_2 \mathbf{h}^{(1)} + \boldsymbol{\beta}_2)\right), \tag{4.9}$$

with $\boldsymbol{\Omega}_2 \in \mathbb{R}^{128 \times 256}$ and $\boldsymbol{\beta}_2 \in \mathbb{R}^{128}$. Dropout is applied with a probability of 0.2 to randomly deactivate neurons during training, enhancing generalization.

The third hidden layer is defined similarly:

$$\mathbf{h}^{(3)} = \text{Dropout}\left(\text{ReLU}(\boldsymbol{\Omega}_3 \mathbf{h}^{(2)} + \boldsymbol{\beta}_3)\right), \tag{4.10}$$

where $\boldsymbol{\Omega}_3 \in \mathbb{R}^{64 \times 128}$ and $\boldsymbol{\beta}_3 \in \mathbb{R}^{64}$.

Finally, the output layer computes the predicted reward:

$$\hat{r}_0 = \boldsymbol{\Omega}_4 \mathbf{h}^{(3)} + \boldsymbol{\beta}_4, \tag{4.11}$$

where $\boldsymbol{\Omega}_4 \in \mathbb{R}^{1 \times 64}$ and $\boldsymbol{\beta}_4 \in \mathbb{R}$. This scalar output represents the expected performance (e.g., achievable sum-rate) for the given input system configuration.

Each $\boldsymbol{\Omega}_l$ denotes the weight matrix and $\boldsymbol{\beta}_l$ the bias vector for the l-th layer of the neural network, with $l \in \{1, 2, 3, 4\}$. The ReLU activation function introduces

non-linearity, allowing the network to learn complex mappings from input features to output reward. The dropout layers help prevent overfitting by randomly omitting nodes during training.

The network is trained using the Adam optimizer with a learning rate of 10^{-4}, mini-batch size of 32, and over 200 epochs. The loss function used is the mean squared error (MSE) between the predicted and true reward values, promoting precise regression performance for joint blocklength and resource optimization.

4.3.2.1 Loss Function and Training Setup

The model is trained using mean squared error (MSE):

$$\mathcal{L} = \frac{1}{L}\sum_{i=1}^{L}(\hat{r}_0^{(i)} - r_0^{(i)})^2. \tag{4.12}$$

where L is the number of training samples, $\hat{r}_0^{(i)}$ is the predicted reward for the i-th sample, and $r_0^{(i)}$ is the true reward for the i-th sample.

Adam optimizer is used with a learning rate of 10^{-4}, 200 epochs, batch size 32, and validation every 30 iterations.

4.4 Gradient-Based Learning Algorithm

The proposed optimization strategy follows an iterative gradient-based learning framework designed to jointly optimize the beamforming matrix $\mathbf{W}$, the FC-RIS scattering matrix $\mathbf{\Theta}$, and the blocklength vector $\mathbf{c} = [c_1, c_2, \ldots, c_K]$ in a fully connected RIS-aided URLLC system.

Initially, the system parameters $\mathbf{W}$, $\mathbf{\Theta}$, and $\mathbf{c}$ are randomly initialized within feasible regions that satisfy power, latency, and blocklength constraints. These parameters are then iteratively refined over a predefined number of training epochs. In each epoch,

the following steps are performed:

1. **SINR Computation:** For each user $k \in \{1, 2, \ldots, K\}$, the signal-to-interference-plus-noise ratio (SINR) SINR_k is computed. This includes contributions from both the direct BS-to-UE link and the RIS-assisted indirect path.

2. **FBL Rate Calculation:** Based on the SINR, the finite blocklength achievable rate R_k for each user is evaluated using the Polyanskiy formula. This rate considers blocklength constraints and the target error probability ϵ_k as:

$$R_k = c_k \log_2(1 + \text{SINR}_k) - Q^{-1}(\epsilon_k)\sqrt{c_k V(\text{SINR}_k)} + \log_2(c_k), \tag{4.13}$$

   where $V(\text{SINR}_k)$ is the channel dispersion function.

3. **System Reward Computation:** The total system reward is defined as the sum of all users' FBL rates:

$$R = \sum_{k=1}^{K} R_k. \tag{4.14}$$

4. **Gradient-Based Updates:** The gradients of the reward function R are computed with respect to $\mathbf{W}$, $\mathbf{\Theta}$, and $\mathbf{c}$. These gradients are used to update the parameters via the Adam optimizer. The optimizer adapts learning rates individually for each parameter and supports momentum through exponential moving averages. Optionally, gradient clipping is applied to stabilize training.

5. **Iteration and Convergence:** The process is repeated for the specified number of epochs or until convergence is observed, i.e., when the change in the reward across epochs falls below a threshold.

The final output of this optimization procedure consists of the optimized beamforming matrix $\mathbf{W}^*$, the fully connected RIS scattering matrix $\mathbf{\Theta}^*$, and the blocklength

allocation vector $\mathbf{c}^*$. These parameters represent the best joint configuration found through the gradient-based iterative process. Once obtained, they are forwarded to the neural network-based joint allocation module, which performs additional fine-tuning to further optimize the blocklength and overall resource allocation strategy for improved system performance.

The proposed framework integrates gradient-based learning with deep neural networks for efficient optimization of FC-RIS-assisted URLLC systems. By exploiting differentiable metrics and learning-based inference, it provides scalable performance improvements in complex communication environments.

Chapter 5

Hybrid CNN-LSTM + SCA Optimization Framework

5.1 Introduction

The optimization problem formulated in Chapter 3 is inherently complex due to its high-dimensional, non-convex nature. The coupling between beamforming vectors, blocklength allocations, and the FC-RIS scattering matrix presents significant challenges for conventional optimization techniques. To tackle this, we propose a hybrid optimization approach that integrates model-based SCA for tractable sub-problems with a DL architecture based on convolutional and recurrent neural networks (CNN-LSTM) to predict the RIS scattering matrix.

5.2 Proposed Method

The proposed method is structured into two interleaved components:

- **Beamforming and Blocklength Optimization:** Using the Tchebyshev method for problem reformulation and solving iteratively through SCA.

- **FC-RIS Optimization:** A CNN-LSTM neural network learns the mapping from channel state information (CSI) to the optimal RIS scattering matrix $\boldsymbol{\Theta}$.

This alternation allows each component to focus on a tractable subproblem, improving both convergence and scalability.

5.2.1 Tchebyshev-Based Reformulation of the Objective Function

The joint optimization of the beamforming matrix (i.e., power allocation) and blocklength configuration follows the SCA methodology introduced in [14]. While the original work in [14] addresses the problem under a SC-RIS architecture, we extend this approach to handle the more complex interactions in FC-RIS systems. The additional non-linearity and inter-element coupling introduced by the FC-RIS configuration demand modified formulations for effective optimization, which we incorporate into our alternating framework.

To handle the non-convex and multi-objective nature of the original problem involving beamforming, blocklength, and RIS scattering matrix optimization, we employ the Tchebyshev scalarization method [22]. This approach allows us to convert the multi-objective problem into a tractable single-objective form by introducing an auxiliary variable μ, and a non-negative weight parameter, Tchebyshev coefficient, $\lambda \in [0, 1]$ that reflects the decision maker's preference between the objectives.

The reformulated problem is given by:

$$\textbf{P2:} \quad \min_{\mathbf{w},\mathbf{c},\boldsymbol{\theta},t} \quad t, \tag{5.1}$$

subject to:

$$\text{C1–C3 (original constraints)}, \tag{5.2}$$

$$\tilde{\text{C}}1: \quad \frac{\lambda}{R^*_{\text{total}}}(R^*_{\text{total}} - R_{\text{total}}(\mathbf{w}, \mathbf{c}, \boldsymbol{\theta})) \leq t, \tag{5.3}$$

$$\tilde{\text{C}}2: \quad \frac{1-\lambda}{c^*_{\text{total}}}(c_{\text{total}}(\mathbf{c}) - c^*_{\text{total}}) \leq t, \tag{5.4}$$

where:

- t is the auxiliary optimization variable.
- R^*_{total} and c^*_{total} are the utopia points (i.e., the ideal best values) of the total achievable FBL sumrate and the total blocklength, respectively.
- $R_{\text{total}}(\cdot)$ and $c_{\text{total}}(\cdot) = \sum_{k=1}^{K} c_k$ are the actual total FBL rate and blocklength values under the current allocation.

The utopia point c^* can be trivially computed as $\sum_{k=1}^{K} c_k^{\min}$ since the minimization of total blocklength subject only to constraints C1–C3 yields this result. The value of R^* is computed by solving the original problem with the blocklength objective excluded.

This scalarized problem **P2** is then solved using an alternating optimization approach, where beamforming and blocklength are optimized via SCA, and the RIS scattering matrix is learned via the CNN-LSTM model described in subsequent sections.

5.2.2 Beamforming Optimization (Power Allocation)

Given a fixed blocklength vector $\mathbf{c}^{(i)}$ and RIS matrix $\boldsymbol{\theta}^{(i)}$, the beamforming subproblem reduces to:

$$\max_{\mathbf{w}_k} \quad R_{\text{total}}(\mathbf{w}_k, \mathbf{c}^{(i)}, \boldsymbol{\theta}^{(i)}), \tag{5.5}$$

$$\text{s.t.} \quad \sum_{k=1}^{K} \|\mathbf{w}_k\|_2^2 \leq P_{\text{total}}. \tag{5.6}$$

In our model, the base station applies maximal ratio transmission (MRT) precoding for each user, where the MRT beamforming vector is defined as:

$$\mathbf{w}_k^{\text{MRT}} = \frac{\mathbf{h}_k}{\|\mathbf{h}_k\|}, \tag{5.7}$$

where $\mathbf{h}_k$ is the effective channel of user k. Let p_k denote the transmit power allocated to user k, i.e., $\mathbb{E}[|s_k[t]|^2] = p_k$. Then, the overall beamforming matrix $\mathbf{W}$ is given by:

$$\mathbf{W} = [\sqrt{p_1} \cdot \mathbf{w}_1^{\text{MRT}}, \sqrt{p_2} \cdot \mathbf{w}_2^{\text{MRT}}, \ldots, \sqrt{p_K} \cdot \mathbf{w}_K^{\text{MRT}}]. \tag{5.8}$$

The total rate R_{total} is expressed as:

$$R_{\text{total}}(\mathbf{p}, \mathbf{c}, \boldsymbol{\theta}) = \tilde{R}_t^+(\mathbf{p}, \mathbf{c}, \boldsymbol{\theta}) - \tilde{R}_t^-(\mathbf{p}, \mathbf{c}, \boldsymbol{\theta}), \tag{5.9}$$

where:

$$\tilde{R}_t^+(\mathbf{p}, \mathbf{c}, \boldsymbol{\theta}) = \sum_{k=1}^{K} c_k \log_2 \left(I_k(\mathbf{p}, \boldsymbol{\theta}) + p_k |\mathbf{d}_{k,k} + \boldsymbol{\theta}^H \mathbf{r}_{k,k}|^2 \right) + \log_2(c_k), \tag{5.10}$$

$$\tilde{R}_t^-(\mathbf{p}, \mathbf{c}, \boldsymbol{\theta}) = \sum_{k=1}^{K} \left(c_k \log_2(I_k(\mathbf{p}, \boldsymbol{\theta})) + \frac{c_k}{\ln 2} Q^{-1}(\epsilon_k) \right). \tag{5.11}$$

Here, $\mathbf{p}, \mathbf{c}, \boldsymbol{\theta}$ are the transmit power vector, blocklength allocation vector, and FC-RIS scattering matrix vector, respectively. The term $\mathbf{r}_{k,k}$ denotes the effective reflected channel at user k given by:

$$\mathbf{r}_{k,k} = \tilde{\mathbf{H}}_k \mathbf{w}_k^{\text{MRT}}, \tag{5.12}$$

where $\tilde{\mathbf{H}}_k$ is the cascaded BS-RIS-UE channel for user k. Using SCA, we approximate $\tilde{R}^-$ using a first-order Taylor expansion around $\mathbf{p}^{(i)}$:

$$\hat{R}_{\text{total}}(\mathbf{w}) = \tilde{R}^+(\mathbf{w}) - \tilde{R}^-(\mathbf{w}^{(i)}) - \nabla_{\mathbf{w}} \tilde{R}^-(\mathbf{w}^{(i)})^T (\mathbf{w} - \mathbf{w}^{(i)}). \tag{5.13}$$

This convex subproblem is solved iteratively.

5.2.3 Blocklength Optimization

With the beamforming matrix $\mathbf{w} = \mathbf{w}^{(i)}$ and RIS configuration $\boldsymbol{\theta} = \boldsymbol{\theta}^{(i)}$ fixed from the previous iteration, the blocklength allocation vector $\mathbf{c}$ is optimized by solving the following sub-problem:

$$\min_{\mathbf{c},t} \quad t \tag{5.14a}$$

$$\text{subject to:} \quad \text{C1 (feasibility constraints)}, \tag{5.14b}$$

$$\tilde{\text{C}}2: \quad \frac{1-\lambda}{c^*}(c^* - \sum_{k=1}^{K} c_k) \leq t, \tag{5.14c}$$

$$\tilde{\text{C}}1: \quad \bar{R}_t(\mathbf{p}^{(i)}, \mathbf{c}, \boldsymbol{\theta}^{(i)}) - \tilde{R}_t^{+}(\mathbf{p}^{(i)}, \mathbf{c}, \boldsymbol{\theta}^{(i)}) \geq R^*(1-t). \tag{5.14d}$$

Here, $\bar{R}_t(\cdot)$ represents the SCA-based approximation of the concave component $\tilde{R}_t^{-}(\cdot)$, and R^* is the utopia point corresponding to the maximum achievable total rate. Following the approach of [14], the concave part $\tilde{R}_t^{-}(\mathbf{p}^{(i)}, \mathbf{c}, \boldsymbol{\theta}^{(i)})$ is upper bounded using a first-order Taylor expansion:

$$\tilde{R}_t^{-}(\mathbf{p}^{(i)}, \mathbf{c}, \boldsymbol{\theta}^{(i)}) \leq \sum_{k=1}^{K} Q^{-1}(\epsilon_k) \frac{\sqrt{c_k^{(i)} V_k(\gamma_k)}}{2} \left(1 + \frac{c_k}{c_k^{(i)}}\right), \tag{5.15}$$

resulting in the convex approximation:

$$\bar{R}_t(\mathbf{p}^{(i)}, \mathbf{c}, \boldsymbol{\theta}^{(i)}) = \tilde{R}_t^{+}(\mathbf{p}^{(i)}, \mathbf{c}, \boldsymbol{\theta}^{(i)}) - \text{upper bound of } \tilde{R}_t^{-}. \tag{5.16}$$

This leads to a convex optimization problem that can be efficiently solved using convex solvers such as CVX. The method ensures that the finite blocklength (FBL) rate is maximized while satisfying system constraints, and is iteratively refined starting from the feasible point $\mathbf{c}^{(i)}$.

The formulation is inspired by and extends the method introduced in [14] to accommodate the FC-RIS architecture.

5.2.4 CNN-LSTM-Based FC-RIS Optimization

To optimize the FC-RIS scattering matrix $\mathbf{\Theta} \in \mathbb{C}^{M \times M}$, we propose a CNN-LSTM deep neural network that learns a mapping from the system state, including channel state information (CSI), power allocation, and blocklength allocation, to the optimal RIS configuration. This hybrid neural architecture combines spatial and temporal feature extraction mechanisms, enabling real-time inference for dynamic URLLC scenarios.

5.2.4.1 Input and Architecture Overview

The network accepts the following composite input:

- **Channel Information:** The direct BS-to-UE channel matrix $\mathbf{H} \in \mathbb{C}^{M \times K}$ and the RIS-to-UE channel vectors $\mathbf{h}_k \in \mathbb{C}^{N \times 1}$ for each UE k.
- **Power Allocation:** Transmit power vector $\mathbf{p} = [p_1, p_2, \ldots, p_K]$.
- **Blocklength Allocation:** Codeword blocklength vector $\mathbf{c} = [c_1, c_2, \ldots, c_K]$.

These are concatenated and flattened into a sequence input of size $N \times M + N \times K + K + K$.

5.2.4.2 Convolutional Feature Extraction

The real and imaginary components of the CSI matrices are separated and concatenated along the input channel dimension. This real-valued sequence is passed through two 1D convolutional layers:

- **Conv1D Layers:** Each layer uses 128 filters and a kernel size optimized for the data dimensionality.

- **Activation:** ReLU (Rectified Linear Unit) is used after each convolution to introduce non-linearity.

This stage captures local spatial dependencies and signal patterns inherent in CSI and allocation vectors.

The operations in the l-th convolutional layer are:

$$\mathbf{F}^{(l)} = \text{ReLU}(\text{BN}_l(\mathbf{W}_{cnn}^{(l)} * \mathbf{F}^{(l-1)} + \mathbf{b}_{cnn}^{(l)})), \tag{5.17}$$

where:

- $*$: 1D convolution,
- $\mathbf{W}_{cnn}^{(l)}, \mathbf{b}_{cnn}^{(l)}$: kernel weights and biases,
- BN_l: batch normalization at layer l,
- $\mathbf{F}^{(0)}$: input sequence.

5.2.4.3 LSTM Temporal Modeling

The CNN output is flattened and forwarded to a two-layer LSTM module to model temporal or contextual relationships:

- **First LSTM Layer:** 256 hidden units.
- **Second LSTM Layer:** 128 hidden units.
- **Dropout:** Applied to prevent overfitting.
- **Activation:** ReLU is applied post-activation in each LSTM cell.

Each LSTM cell is updated using the following equations:

$$\mathbf{i}_t = \sigma(\mathbf{W}_{lstm}^{(i)}\mathbf{x}_t + \mathbf{U}_{lstm}^{(i)}\mathbf{h}_{t-1} + \mathbf{b}_{lstm}^{(i)}), \tag{5.18}$$

$$\mathbf{f}_t = \sigma(\mathbf{W}_{lstm}^{(f)}\mathbf{x}_t + \mathbf{U}_{lstm}^{(f)}\mathbf{h}_{t-1} + \mathbf{b}_{lstm}^{(f)}), \tag{5.19}$$

$$\mathbf{o}_t = \sigma(\mathbf{W}_{lstm}^{(o)}\mathbf{x}_t + \mathbf{U}_{lstm}^{(o)}\mathbf{h}_{t-1} + \mathbf{b}_{lstm}^{(o)}), \tag{5.20}$$

$$\tilde{\mathbf{c}}_t = \tanh(\mathbf{W}_{lstm}^{(c)}\mathbf{x}_t + \mathbf{U}_{lstm}^{(c)}\mathbf{h}_{t-1} + \mathbf{b}_{lstm}^{(c)}), \tag{5.21}$$

$$\mathbf{c}_t = \mathbf{f}_t \odot \mathbf{c}_{t-1} + \mathbf{i}_t \odot \tilde{\mathbf{c}}_t, \tag{5.22}$$

$$\mathbf{h}_t = \mathbf{o}_t \odot \tanh(\mathbf{c}_t), \tag{5.23}$$

where:

- $\mathbf{x}_t \in \mathbb{R}^d$: Flattened CNN feature vector at time t.
- $\mathbf{i}_t, \mathbf{f}_t, \mathbf{o}_t \in \mathbb{R}^{d_h}$: Input, forget, and output gates.
- $\mathbf{c}_t \in \mathbb{R}^{d_h}$: Cell memory state at time t.
- $\mathbf{h}_t \in \mathbb{R}^{d_h}$: LSTM hidden state at time t.
- $\tilde{\mathbf{c}}_t$: Candidate cell state.
- $\mathbf{W}_{lstm}^{(*)}, \mathbf{U}_{lstm}^{(*)}, \mathbf{b}_{lstm}^{(*)}$: Trainable weight matrices and bias vectors.
- $\sigma(\cdot)$: Sigmoid activation function.
- $\tanh(\cdot)$: Hyperbolic tangent activation function.
- d_h: Dimensionality of the hidden state.

and $\odot$ denotes element-wise multiplication.

5.2.4.4 Fully Connected Output and RIS Mapping

The final hidden state $\mathbf{h}_T \in \mathbb{R}^{128}$ from the LSTM layer is projected using a fully connected layer:

$$\mathbf{\Theta}_{\text{pred}} = \tanh(\mathbf{W}_{fc}^{(out)}\mathbf{h}_T + \mathbf{b}_{fc}^{(out)}), \tag{5.24}$$

where:

- $\mathbf{W}_{fc}^{(out)} \in \mathbb{R}^{M^2 \times 128}$: Output layer weights.
- $\mathbf{b}_{fc}^{(out)} \in \mathbb{R}^{M^2}$: Output layer biases.
- $\mathbf{\Theta}_{\text{pred}} \in \mathbb{R}^{M \times M}$: Predicted real-valued RIS matrix.

The tanh activation ensures values in $[-1, 1]$, scalable to phase angles in $[-\pi, \pi]$.

5.2.4.5 Scattering Matrix Computation

The predicted $\mathbf{\Theta}_{\text{pred}}$ is used to construct the reactance matrix $\mathbf{X}$, from which the scattering matrix is derived as:

$$\mathbf{\Theta} = (j\mathbf{X} + Z_0\mathbf{I})^{-1}(j\mathbf{X} - Z_0\mathbf{I}). \tag{5.25}$$

5.2.4.6 Training and Inference

- **Loss Function:** Mean Squared Error (MSE) between predicted and target phase matrices.
- **Optimizer:** Adam optimizer with exponential learning rate decay.
- **Training:** 200 epochs, mini-batch size of 64.

5.2.4.7 Model Mapping Equation

The final deep learning model is represented as:

$$\boldsymbol{\Theta}_{\text{pred}} = \tanh\left(f_{\text{CNN-LSTM}}(\mathbf{H}, \mathbf{h}_k, \mathbf{p}, \mathbf{c})\right), \tag{5.26}$$

where $f_{\text{CNN-LSTM}}(\cdot)$ encapsulates all network layers from convolution through LSTM to the fully connected output.

This deep learning approach enables fast and data-adaptive optimization of FC-RIS configurations, significantly reducing the complexity of solving high-dimensional, non-convex optimization problems in URLLC environments.

5.2.5 Alternating Optimization Algorithm

The proposed optimization approach employs an iterative alternating strategy to efficiently solve the complex joint problem of beamforming, blocklength allocation, and RIS configuration. The method begins by initializing the beamforming matrix $\mathbf{W}$, the FC-RIS scattering matrix $\boldsymbol{\Theta}$, and the blocklength vector $\mathbf{c}$. These initial values may be randomly chosen or derived from heuristic rules.

In each iteration, the algorithm proceeds in two main stages. First, with the current RIS configuration $\boldsymbol{\Theta}$ fixed, the beamforming vectors and blocklengths are updated using the SCA technique. This step addresses the power and latency constraints while maximizing the FBL rate. The convexified sub-problems for beamforming and blocklengths are solved iteratively until a local optimal solution is obtained.

Next, keeping the updated values of $\mathbf{W}$ and $\mathbf{c}$ fixed, the RIS scattering matrix $\boldsymbol{\Theta}$ is predicted using the trained CNN-LSTM deep learning model. This model takes as input the CSI and outputs the optimal FC-RIS configuration that improves signal propagation and interference management.

After both stages are complete, the algorithm checks for convergence. This can be assessed based on whether the change in the objective function between successive iterations falls below a predefined threshold, or after a maximum number of iterations is reached. If the convergence condition is not satisfied, the updated variables are used as the new inputs, and the process repeats.

Upon convergence, the algorithm outputs the final optimized variables: the beamforming matrix $\mathbf{W}^*$, the blocklength allocation vector $\mathbf{c}^*$, and the FC-RIS scattering matrix $\boldsymbol{\Theta}^*$. This alternating optimization procedure efficiently balances computational complexity with performance accuracy, and is well-suited for real-time application in dynamic wireless environments.

5.3 Conclusion

This chapter presented a hybrid optimization framework combining SCA with a CNN-LSTM deep learning model to solve the joint optimization of beamforming, blocklength, and RIS configuration. By leveraging both theoretical and data-driven tools, the framework offers an effective and scalable solution for URLLC under FC-RIS architectures.

Chapter 6

Simulation Setup and Performance Evaluation

6.1 Simulation Results for Gradient-Based DL Method

6.1.1 Simulation Setup

To evaluate the performance of the proposed gradient-based deep learning optimization framework, extensive simulations were conducted using the parameters listed in Tables 6.1 and 6.2. The simulation involves a downlink transmission scenario with four single-antenna UEs located at coordinates (114, 40)m, (132, 44)m, (148, 35)m, and (164, 45)m, respectively. The BS is equipped with $M = 4$ antennas and positioned at the origin. A fully connected RIS with $N = 16$ passive elements is placed at (40, 10)m. The reference impedance of the RIS is set to 50 ohms.

All channels are modeled as Rician fading with a Rician factor of 10, and pathloss exponents are set to 3.5 (BS-to-UE), 2.2 (BS-to-RIS), and 2.2 (RIS-to-UE). A total of 1000 independent channel realizations are used to average the performance metrics

such as SINR and achievable finite blocklength (FBL) rate.

Table 6.1: Gradient-Based DL Network Training Parameters

Parameter	**Value/Description**
Beamforming matrix ($\mathbf{W}$)	4×4 complex matrix, initialized with small random values
RIS Phase Matrix ($\mathbf{\Theta}$)	16×16 matrix, initialized randomly
Block Length Allocation ($\mathbf{c}_k$)	1×4 vector, randomly initialized under constraints
Learning Rate (α)	5×10^{-4}
Optimizer	Adam optimizer
Epochs	200
Gradient Clipping Threshold	0.05
Adam Parameters	$\beta_1 = 0.9$, $\beta_2 = 0.999$, $\epsilon = 10^{-8}$
Batch Size	32

6.1.2 Performance Evaluation

6.1.2.1 Training Convergence

Fig. 6.1 illustrates the evolution of the training loss across iterations for different system architectures. It is evident that the FC-RIS short packet NOMA configuration exhibits a slower and more gradual convergence pattern compared to other schemes. This behavior is attributed to the increased complexity of the FC-RIS design, where each RIS element contributes to the optimization space, leading to a higher-dimensional and more intricate objective landscape. The model must therefore process a richer set of CSI patterns and dynamically optimize more parameters, which inherently demands more computational iterations. Conversely, SC-RIS and no-RIS short packet NOMA configurations demonstrate quicker convergence due to

Table 6.2: Simulation Parameters for DL Algorithm

Parameter	**Value**
Number of UEs (K)	4
Number of BS antennas (M)	4
Number of RIS elements (N)	16
Total transmit power (P_{total})	10 dB
Target BLER (ϵ_{th})	10^{-6}
Noise power density (N_0)	1 dB
Minimum CBL ($c_{\min}$)	10
Total available CBL (C)	100
Bandwidth	0.1 MHz
Reference path loss (PL_0)	-30 dB
Path loss coefficients	BS-UE: 3.5, BS-RIS: 2.2, RIS-UE: 2.2
BS location	[0,0] m
RIS location	[40,10] m

their lower-dimensional design spaces and fewer optimization variables. Additionally, the FC-RIS short packet OMA scenario converges the fastest among all, likely because it does not involve the inter-user interference handling required in NOMA systems, allowing for a simpler and more stable optimization process. These observations are in line with theoretical expectations and emphasize the practical challenges involved in learning-assisted joint optimization under FC-RIS-NOMA conditions.

6.1.2.2 Reward vs. Transmit Power

To evaluate the relationship between system transmit power and achievable FBL rate, we simulate the proposed method across a transmit power range of 10 dB to 30 dB. As shown in Fig. 6.2a, the optimized reward improves monotonically with increasing transmit power due to enhanced SINR for each user. The FC-RIS-enabled

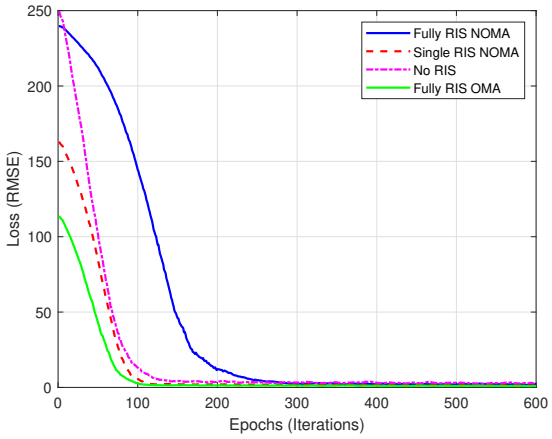

Figure 6.1: Training loss versus number of iterations.

configuration consistently delivers the highest sum-rate among all tested configurations, including SC-RIS and non-RIS baselines. This superior performance highlights the benefits of fine-grained phase adjustment across all RIS elements in the fully connected topology. The curve also shows that while random RIS configurations do offer improvements over no-RIS setups, they are significantly outperformed by both FC-RIS and SC-RIS with optimized phase shift matrices. Notably, the traditional zero-forcing (ZF) beamforming strategy achieves modest rate gains but is clearly suboptimal compared to the proposed hybrid learning-based optimization strategy, which more effectively captures system-level dependencies and constraints. As transmit power increases, the gap between random and optimized RIS configurations also widens, reflecting the compounding benefits of structured optimization in high-SNR regimes.

6.1.2.3 Reward vs. Maximum Blocklength

The impact of available blocklength on system performance is analyzed in Fig. 6.2b, where the total maximum code block length (CBL) is varied from 100 to 200 symbols. The optimized FBL rate increases with larger blocklength allocations, primarily

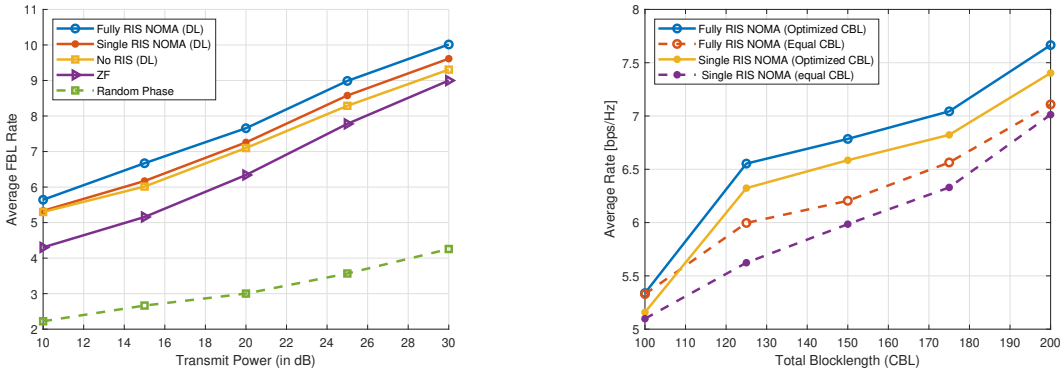

(a) Sumrate vs transmit power

(b) Sumrate vs maximum CBL

Figure 6.2: Comparison of FBL rate under varying system parameters.

because longer codewords reduce decoding error probabilities, thereby improving the achievable data rates. This performance boost is significantly more prominent in the FC-RIS scenario compared to the SC-RIS configuration. The results validate that the FC-RIS offers better adaptability and spatial control, enabling more efficient exploitation of the available codeword symbols. Moreover, we observe that strategies employing equal CBL allocation across users underperform in both RIS architectures, underscoring the necessity for optimized blocklength assignments to maximize spectral efficiency. These trends reaffirm the utility of learning-assisted multi-variable optimization for URLLC under finite blocklength constraints.

6.2 Simulation Results for SCA-CNN-LSTM-Based Method

6.2.1 Simulation Setup

The CNN-LSTM-based optimization is evaluated using the same multi-user RIS-assisted short packet system, where the FC-RIS assists the BS in delivering data to

four UEs. The RIS has 16 elements and a reference impedance of 50 ohms. The base station is placed at (180, 0) m, and the RIS is at (200, 0) m. The user positions remain unchanged. Channels are assumed to undergo Rician fading with factor 10, and the simulations use 1000 different random realizations.

Table 6.3: CNN-LSTM-Based DL Network Training Parameters

Component	**Description**
CNN Layers	2 convolutional layers with ReLU activations
LSTM Network	2 LSTM layers (256 and 128 units) with dropout
Output Layer	Fully connected + `tanh()` activation
Beamforming Initialization	4×4 complex matrix, power-normalized
RIS Initialization	Random symmetric 16×16 matrix mapped via impedance formula
CBL Vector ($\mathbf{c}$)	Random in [10, 100], with $\sum c_k \leq 100$
Learning Rate	1×10^{-4}, Adam optimizer
Epochs	200
Batch Size	64
Gradient Clipping	Threshold 0.05

6.2.2 Performance Evaluation

6.2.2.1 Convergence Behavior over Iterations

To evaluate the convergence performance of the proposed CNN-LSTM-assisted SCA framework, we plot the optimized sum-rate over 100 iterations for different benchmark methods, as shown in Fig. 6.3. The proposed CLSTM+SCA method, which combines successive convex approximation for convexified subproblems with CNN-LSTM-

Table 6.4: Simulation Parameters for CNN-LSTM-Based FC-RIS Optimization

Parameter	**Value**
Number of UEs (K)	4
BS antennas (M)	4
RIS elements (N)	16
Transmit power (P_{total})	10 mW
Target BLER	10^{-8}
Noise Power Density	-174 dBm/Hz
Total Bandwidth	2 MHz
Reference Pathloss	-30 dB, -20 dB
Minimum Blocklength	20 symbols
Total CBL (C)	200
Tchebyshev Coefficient (λ)	0.8

based learning for RIS matrix prediction, demonstrates the fastest convergence and highest sum-rate performance. The optimization stabilizes near 30 bits/s/Hz within the first 20 iterations and maintains stable performance thereafter. In comparison, the gradient-based DL method without convexification converges slower and reaches a lower steady-state sum-rate of around 28.5 bits/s/Hz, indicating its limited effectiveness in handling the high non-convexity of RIS-aided systems. The SCA-only approach initially improves rapidly but soon saturates below 28 bits/s/Hz, lacking the generalization capabilities provided by neural prediction models. The SC-RIS case, despite utilizing the same hybrid framework, performs the worst due to architectural limitations in scattering flexibility and demonstrates how FC-RIS offers significant spectral efficiency gains. These trends collectively confirm that the CLSTM+SCA method is more efficient and robust, offering superior convergence and optimized rate performance over alternative schemes. The gap between FC-RIS and SC-RIS cases further

highlights the benefits of precise and tunable RIS control in enhancing URLLC performance under FBL constraints. Our findings are also consistent with related works such as [18] and [14], reinforcing the idea that a hybrid model-based and learning-driven optimization paradigm offers better scalability and real-time adaptability than either approach in isolation.

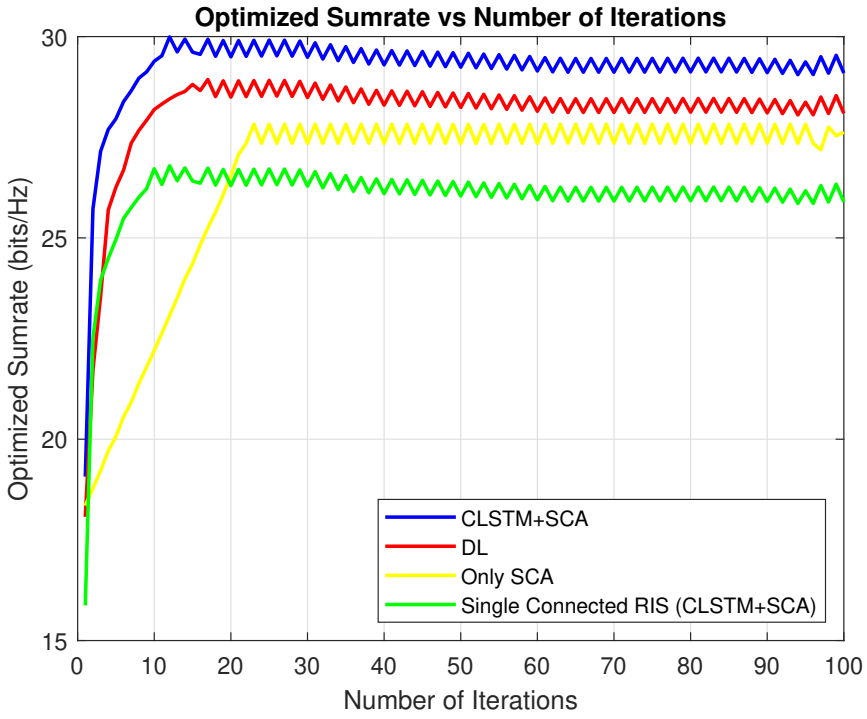

Figure 6.3: Optimized sum-rate (bits/s/Hz) versus number of iterations for various optimization strategies.

6.2.2.2 Optimized Sumrate vs. Transmit Power

Fig. 6.4 illustrates how the average finite FBL rate evolves with increasing transmit power across different RIS configurations. The proposed method, which combines CNN-LSTM-based scattering matrix prediction with SCA-based optimization, achieves the highest performance among all schemes evaluated. As transmit power increases from 10 mW to 25 mW, the FC-RIS configuration optimized with CNN-

LSTM shows a consistently steeper increase in achievable rate compared to both the SC-RIS and the SCA-only variant. Notably, systems using random phase shifts at the RIS perform significantly worse, with the performance gap widening at higher power levels, underscoring the importance of intelligent RIS phase design. The traditional no-RIS scenario lags far behind all RIS-enabled schemes, reaffirming the critical role of RIS in enhancing link quality under FBL constraints. These results emphasize that precise beamforming and phase control—enabled by the CNN-LSTM model—are key to harnessing the full potential of RIS in low-latency communication regimes.

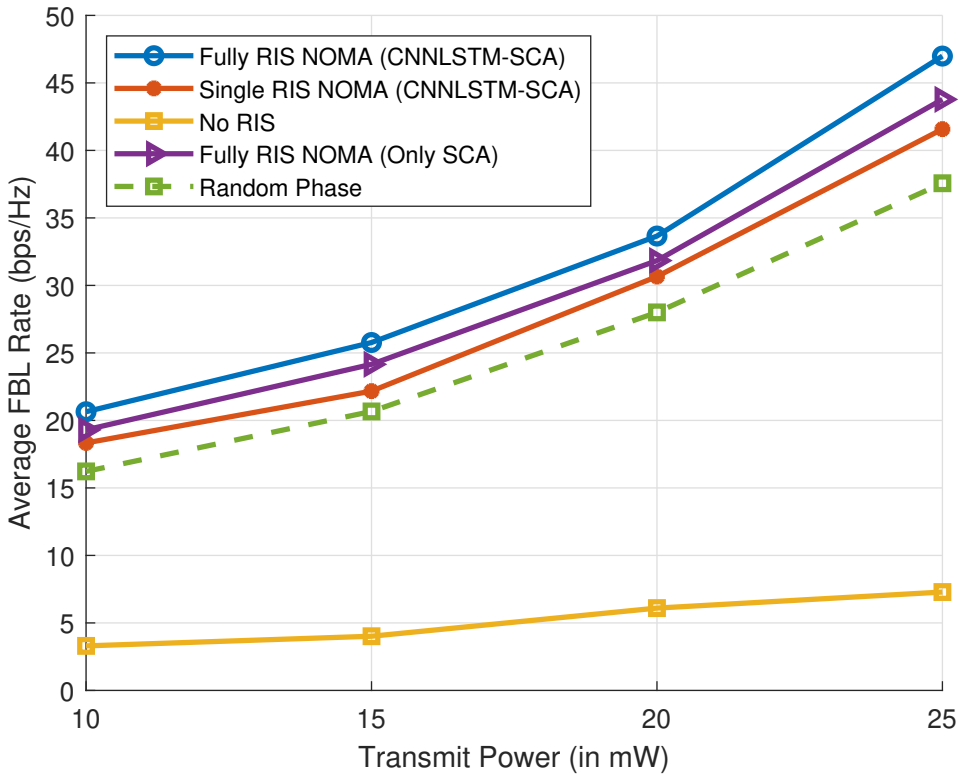

Figure 6.4: Optimized FBL rate as a function of transmit power (in mW).

6.2.2.3 Minimum Required Blocklength vs. Number of UEs

The results in Fig. 6.5a evaluate the system's scalability by examining the minimum required channel blocklength as the number of UEs increases from 2 to 8. A clear upward trend is observed across all configurations, consistent with the growing demand on system resources due to increased user interference and contention. However, the FC-RIS configurations, particularly with a higher number of BS antennas (i.e., $M = 8$), require significantly lower blocklength than other schemes. This advantage becomes increasingly pronounced as the number of users grows, highlighting the proposed method's ability to maintain low-latency communication in dense networks. The SC-RIS-based schemes, while benefiting from RIS assistance, exhibit higher blocklength requirements than their FC-RIS counterparts. Furthermore, systems with random RIS phase shifts consistently require the highest blocklength, indicating inefficient channel utilization in the absence of optimization.

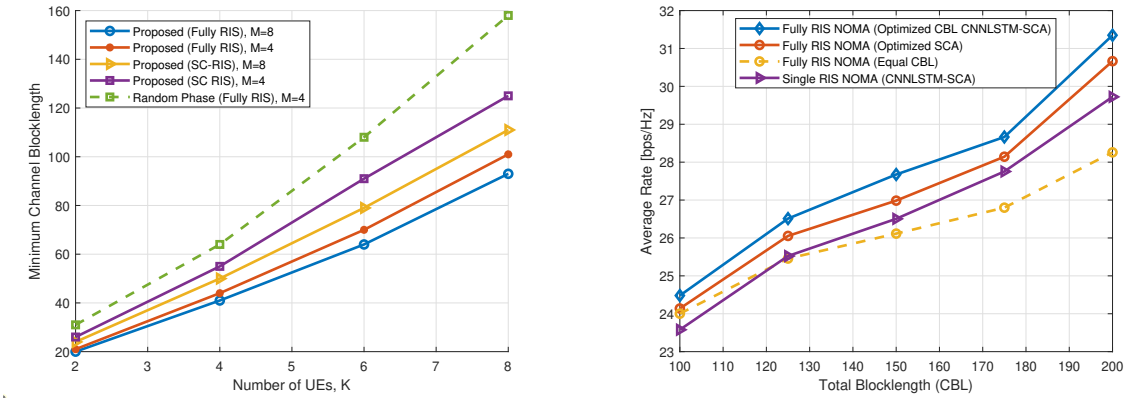

(a) Minimum required blocklength as a function of number of UEs.

(b) Average rate vs. total blocklength for different RIS and allocation strategies.

Figure 6.5: Performance comparison of blocklength and rate under varying conditions.

6.2.2.4 Optimized Sumrate vs. Total Blocklength

Fig. 6.5b presents the variation of average achievable rate with respect to total blocklength, highlighting the effect of both RIS configuration and codeword blocklength allocation strategies. It is evident that increasing the blocklength leads to significant rate improvements across all scenarios, owing to reduced decoding error probability. The CNN-LSTM + SCA framework with FC-RIS and optimized blocklength allocation consistently achieves the best performance, surpassing both equal allocation and SC-RIS cases. Compared to SCA-only optimization, the hybrid method further enhances rate performance, particularly at higher blocklength values. The gap between equal and optimized blocklength allocation becomes increasingly substantial, confirming that blocklength adaptation is crucial for maximizing FBL rates in heterogeneous network environments.

Thus, the SCA-CNN-LSTM approach demonstrates strong capability in managing highly non-convex RIS design problems, producing consistent gains in FBL rate, resource usage, and adaptability. Compared to the gradient-based method, it provides improved scalability and accuracy in high-dimensional optimization under short-packet communication constraints.

6.2.3 Complexity Analysis

6.2.3.1 Gradient-Based Deep Learning Method

The computational complexity of the gradient-based deep learning method is primarily dominated by three components: optimization using the Adam optimizer, gradient clipping, and neural network training.

The Adam optimizer performs parameter updates for the beamforming matrix $\mathbf{W}$, the RIS scattering matrix $\mathbf{\Theta}$, and the user blocklength vector $\mathbf{c}$. The complexity per

update is $O(MK+N^2)$ for $\mathbf{W}$ and $\mathbf{\Theta}$, and $O(K)$ for $\mathbf{c}$. Additionally, gradient clipping, which is a component-wise operation on the gradients, incurs $O(MK + N^2 + K)$ cost per iteration. Letting T denote the number of training iterations, the total complexity for the optimizer becomes:

$$O(T \times (MK + N^2 + K)). \tag{6.1}$$

The neural network consists of multiple fully connected layers applied to an input of size $O(N^2 + MK + K)$, which combines the beamforming vector, RIS phases, and user metrics. Let the network have L layers and each layer have N_l neurons. The forward and backward passes through the network per epoch thus have complexity:

$$O((N^2 + MK + K) \times \sum_{l=1}^{L} N_l). \tag{6.2}$$

If the network is trained over E epochs, the total training complexity becomes:

$$O(E \times (N^2 + MK + K) \times \sum_{l=1}^{L} N_l). \tag{6.3}$$

Combining the optimizer updates and training phases, the total computational complexity of the gradient-based deep learning approach is:

$$O\left(T(MK + N^2 + K) + E(N^2 + MK + K)\sum_{l=1}^{L} N_l\right). \tag{6.4}$$

6.2.3.2 CNN-LSTM + SCA Alternating Optimization Method

The CNN-LSTM + SCA method involves channel estimation, neural network inference, and convex optimization. Each component has a distinct computational footprint.

For channel estimation, the direct BS–UE links and RIS–UE links are estimated with complexity $\mathcal{O}(MK + NK)$.

The CNN-LSTM model receives as input a flattened tensor of size $D = N \cdot M + N \cdot K + 2K$ and produces a phase matrix $\mathbf{\Theta} \in \mathbb{C}^{N \times N}$. For a model with L layers and F neurons per layer, the forward-pass inference complexity is dominated by matrix multiplications and is given by:

$$\mathcal{O}(FD + N^2), \tag{6.5}$$

where N^2 accounts for reshaping and conversion to phase shifts.

SCA-based convex optimization includes two alternating sub-problems per iteration. The power allocation and blocklength allocation steps each involve K optimization variables with quadratic constraints, and both have a per-iteration complexity of:

$$\mathcal{O}(K^3). \tag{6.6}$$

Additionally, computing the FBL rate across K users involves:

$$\mathcal{O}(KM), \tag{6.7}$$

as it includes logarithmic and square root evaluations per user.

Combining all components, the total complexity per iteration of the CNN-LSTM + SCA-based algorithm is:

$$\boxed{\mathcal{O}(MK + NK + FD + N^2 + 2K^3 + KM)}. \tag{6.8}$$

Assuming F and D scale as $O(NM)$, the expression simplifies to:

$$\boxed{\mathcal{O}(MK + NK + N^2M + 2K^3)}. \tag{6.9}$$

6.2.3.3 Comparison and Observations

The above complexity analysis shows that the CNN-LSTM + SCA approach significantly reduces the high computational cost traditionally associated with RIS optimization, such as in full FC-based deep learning ($O(N^3)$) or matrix inversion methods [28].

Table 6.5: Computational Complexity Comparison of Different Methods

Method	**Complexity**
Gradient-Based DL	$O(T(MK + N^2 + K) + E(N^2 + MK + K)\sum N_l)$
CNN-LSTM + SCA	$O(MK + NK + N^2M + 2K^3)$
Deep Learning (FC only)	$O(N^3 + M^3)$
ZF Beamforming [28]	$O(M^3)$
Random RIS Phase	$O(MK)$
RIS with grouping (size g)	$O(MK + \frac{N}{g}K + K^3)$

Although gradient-based methods may appear simpler, their training cost can dominate as the network size grows. In contrast, once trained, the CNN-LSTM model allows faster inference-based decisions with significantly reduced RIS optimization cost compared to naive exhaustive search or traditional matrix decomposition methods. The proposed hybrid architecture offers an effective trade-off between real-time inference, optimization accuracy, and computational burden, making it well-suited for intelligent 6G wireless environments with ultra-low-latency requirements.

Chapter 7

Conclusion and Future Work

This thesis presented a comprehensive study on the optimization of downlink resource allocation in reconfigurable intelligent surface (RIS)-aided ultra-reliable low-latency communication (URLLC) systems under the short packet regime. The primary goal was to enhance system performance, measured by the achievable finite blocklength (FBL) rate, while satisfying practical constraints such as power budgets and strict latency requirements. A joint optimization framework was proposed, targeting the beamforming matrix at the base station (BS), the RIS scattering matrix, and the user-specific codeword blocklengths.

To address the intrinsic non-convexity of the problem, two distinct yet complementary methodologies were developed. The first approach relied on a gradient-based deep learning (DL) model integrated with the Adam optimizer. This method updated the beamforming weights, RIS phases, and blocklengths iteratively using the gradients of the FBL rate as the objective function. The neural network was trained to learn optimal policies based on high-dimensional channel state information and user constraints, offering a scalable and adaptive solution suitable for real-time implementation.

The second method incorporated a hybrid model combining the interpretability of

successive convex approximation (SCA) with the prediction power of a deep learning model. A CNN-LSTM-based architecture was trained to map time-varying CSI to the RIS scattering matrix. The SCA framework was used alternately to solve the convexified sub-problems for beamforming and blocklength optimization. This hybrid CNN-LSTM + SCA framework showed superior performance by leveraging both domain knowledge and data-driven learning.

Extensive simulations were conducted to validate the proposed methods. Results showed that both the gradient-based DL and CNN-LSTM + SCA schemes significantly outperformed conventional baselines, such as random RIS phases, zero-forcing (ZF) beamforming, and equal blocklength allocation strategies. In particular, the CNN-LSTM + SCA framework achieved the highest FBL rates and the lowest required blocklengths across different system configurations. Furthermore, the proposed approach offered robust scalability with respect to the number of users and RIS elements, establishing its applicability in future 6G networks.

The complexity analysis revealed that the CNN-LSTM + SCA method offers a favorable trade-off between performance and computational overhead. Once trained, the CNN-LSTM network allows for efficient inference of the RIS matrix, avoiding the need for exhaustive search or iterative decomposition. Compared to traditional methods, the proposed hybrid architecture achieves high optimization accuracy with moderate computational cost, making it suitable for practical deployment in dynamic environments with stringent latency constraints.

While the proposed approaches deliver substantial improvements in system performance, several open directions remain for future research. First, the current CNN-LSTM model assumes a supervised training environment with perfect ground truth. Future work may explore reinforcement learning or unsupervised learning frameworks

that enable training directly from interaction with the environment, thereby eliminating the need for labeled data.

Second, while this work focused on single-cell MISO systems, extension to multi-cell and multi-RIS networks presents both challenges and opportunities. Inter-cell interference, RIS cooperation, and distributed optimization schemes need to be carefully addressed. Incorporating graph neural networks or federated learning paradigms could be promising directions to tackle such scalability issues.

Third, energy efficiency and hardware impairments were not considered in this study. Practical implementations of RISs often suffer from hardware limitations such as discrete phase shifts, quantization noise, and imperfect channel estimation. Integrating these real-world constraints into the optimization framework is essential for reliable system design.

Finally, the integration of RIS with emerging technologies such as cell-free massive MIMO, and mmWave communications remains largely unexplored in the context of short packet URLLC. Exploring RIS-aided NOMA in high-frequency bands under FBL constraints could significantly enhance network reliability and capacity.

In conclusion, this thesis provides a solid foundation for intelligent RIS optimization under FBL constraints and opens several new avenues for innovation in future wireless communication systems.

Bibliography

[1] M. Bennis, M. Debbah, and H. V. Poor, "Ultra-reliable and low-latency wireless communication: Tail, risk and scale," *Proceedings of the IEEE*, vol. 106, no. 10, pp. 1834–1853, 2018.

[2] Y. Polyanskiy, H. V. Poor, and S. Verdu, "Channel coding rate in the finite blocklength regime," *IEEE Transactions on Information Theory*, vol. 56, no. 5, pp. 2307–2359, 2010.

[3] Z. Ding, Y. Liu, H. Choi, M. Elkashlan, C.-L. I, and H. V. Poor, "Non-orthogonal multiple access for 5G and beyond," *IEEE Journal on Selected Areas in Communications*, vol. 35, no. 10, pp. 2181–2195, 2017.

[4] C. Huang, A. Zappone, G. C. Alexandropoulos, M. Debbah, and C. Yuen, "Reconfigurable intelligent surfaces for energy efficiency in wireless communication," *IEEE Transactions on Wireless Communications*, vol. 18, no. 8, pp. 4157–4170, 2019.

[5] M. Di Renzo, M. Debbah, D. N. Phan-Huy, A. Zappone, M.-S. Alouini, C. Yuen, J. De Rosny, S. A. Tretyakov, M. F. Flanagan, and M. Elkashlan, "Smart radio environments empowered by reconfigurable AI meta-surfaces: An idea whose time has come," *EURASIP Journal on Wireless Communications and Networking*, vol. 2020, no. 1, pp. 1–20, 2020.

[6] L. Dai, R. Jiao, F. Adachi, H. V. Poor, and L. Hanzo, "Deep learning for wireless communications: An emerging interdisciplinary paradigm," *IEEE Wireless Communications*, vol. 27, no. 4, pp. 133–139, 2020.

[7] R. Hashemi, S. M. Ali, N. H. Mahmood, and M. Latva-aho, "Deep reinforcement learning for practical phase-shift optimization in RIS-aided MISO URLLC systems," *IEEE Internet of Things Journal*, vol. 10, no. 10, pp. 8931–8943, 2023.

[8] C. Huang, A. Zappone, G. C. Alexandropoulos, M. Debbah, and C. Yuen, "Reconfigurable intelligent surfaces for energy efficiency in wireless communication," *IEEE Transactions on Wireless Communications*, vol. 18, no. 8, pp. 4157–4170, 2019.

[9] Q. Wu and R. Zhang, "Towards smart and reconfigurable environment: Intelligent reflecting surface aided wireless network," *IEEE Communications Magazine*, vol. 58, no. 1, pp. 106–112, 2019.

[10] S. Zhang and R. Zhang, "Intelligent reflecting surface-aided wireless communications: A tutorial," *IEEE Communications Surveys & Tutorials*, vol. 23, no. 2, pp. 1107–1156, 2021.

[11] H. Li, S. Shen, and B. Clerckx, "Beyond diagonal reconfigurable intelligent surfaces: From transmitting and reflecting modes to single-, group-, and fully-connected architectures," *IEEE Transactions on Wireless Communications*, vol. 22, no. 4, pp. 2311–2324, 2023.

[12] M. Bennis, M. Debbah, and H. V. Poor, "Ultra-reliable and low-latency wireless communication: Tail, risk and scale," *Proceedings of the IEEE*, vol. 106, no. 10, pp. 1834–1853, 2018.

[13] C. Shi, Y. Zhu, X. Li, and A. Schmeink, "Energy-optimised design for secure-reliability within finite blocklength regime," *2024 19th International Symposium on Wireless Communication Systems (ISWCS)*, pp. 1–6, 2024.

[14] R. Hashemi, S. Ali, N. H. Mahmood, and M. Latva-Aho, "Joint Sum Rate and Blocklength Optimization in RIS-Aided Short Packet URLLC Systems," *IEEE Communications Letters*, vol. 26, no. 8, pp. 1838–1842, 2022.

[15] H. Ren, K. Wang, and C. Pan, "Intelligent reflecting surface-aided URLLC in a factory automation scenario," *IEEE Transactions on Communications*, vol. 70, no. 1, pp. 707–723, 2022.

[16] H. Yang, X. He, H. Wang, Y. Huang, and J. Song, "RIS-assisted URLLC under finite blocklength: Optimization and deep reinforcement learning," *IEEE Journal on Selected Areas in Communications*, vol. 39, no. 7, pp. 1866–1880, 2021.

[17] S. Kurma, T. A. Lestari, K. Singh, A. Paul, and S. Mumtaz, "Active RIS in digital twin-based URLLC IoT networks: Fully-connected versus sub-connected?" *IEEE Transactions on Wireless Communications*, vol. 23, no. 9, pp. 12 354–12 367, 2024.

[18] F. Zhu, X. Wang, C. Huang, Z. Yang, X. Chen, A. Alhammadi, Z. Zhang, C. Yuen, and M. Debbah, "Robust beamforming for RIS-aided communications: Gradient-based manifold meta learning," *IEEE Transactions on Wireless Communications*, 2024.

[19] L. Dai, R. Jiao, F. Adachi, H. V. Poor, and L. Hanzo, "Deep learning for wireless communications: An emerging interdisciplinary paradigm," *IEEE Wireless Communications*, vol. 27, no. 4, pp. 133–139, 2020.

[20] C. Nguyen, T. M. Hoang, and A. A. Cheema, "Channel estimation using CNN-LSTM in RIS-NOMA assisted 6G network," *IEEE Transactions on Machine Learning in Communications and Networking*, vol. 1, pp. 43–60, 2023.

[21] R. Hashemi, S. Ali, N. H. Mahmood, and M. Latva-Aho, "Deep reinforcement learning for practical phase-shift optimization in RIS-aided MISO URLLC systems," *IEEE Internet of Things Journal*, vol. 10, no. 10, pp. 8931–8943, 2023.

[22] R. Marler and J. Arora, "Survey of Multi-Objective Optimization Methods for Engineering," *Structural and Multidisciplinary Optimization*, vol. 26, pp. 369–395, 2004.

[23] X. Ou, X. Xie, H. Lu, and H. Yang, "Channel blocklength minimization in MU-MISO nonorthogonal multiple access for URLLC services," *IEEE Systems Journal*, vol. 18, no. 1, pp. 36–39, 2024.

[24] H. Shen, W. Xu, S. Gong, Z. He, and C. Zhao, "Secrecy rate maximization for intelligent reflecting surface assisted multi-antenna communications," *IEEE Communications Letters*, vol. 23, no. 9, pp. 1488–1492, 2019.

[25] A. Ranjha and G. Kaddoum, "URLLC-enabled by laser powered UAV relay: A quasi-optimal design of resource allocation, trajectory planning and energy harvesting," *IEEE Transactions on Vehicular Technology*, vol. 71, no. 1, pp. 753–765, 2022.

[26] S. Shen, B. Clerckx, and R. Murch, "Modeling and Architecture Design of Reconfigurable Intelligent Surfaces Using Scattering Parameter Network Analysis," *IEEE Transactions on Wireless Communications*, pp. 1–1, 2021.

[27] Z. Wang and B. Clerckx, "RIS-aided dual-functional radar and communications beamforming design," Master's thesis, Imperial College London, London, UK, Sep. 2021.

[28] Q. Wu and R. Zhang, "Intelligent Reflecting Surface Enhanced Wireless Network via Joint Active and Passive Beamforming," *IEEE Transactions on Wireless Communications*, vol. 18, no. 11, pp. 5394–5409, 2019.